Metal-insulator transition in Si inversion layers in the extreme quantum limit

V. T. Dolgopolov, G. V. Kravchenko, and A. A. Shashkin
Institute of Solid State Physics, Chernogolovka, 142432 Moscow District, Russia

S. V. Kravchenko
Physics Department, University of Nottingham, Nottingham NG7 2RD, United Kingdom
and Institute for High Pressure Physics, Troitsk, 142092 Moscow District, Russia
(Received 27 March 1992; revised manuscript received 9 July 1992)

We report magnetotransport data of an insulating phase in silicon inversion layers in the extreme quantum limit at a Landau-level filling factor of $\nu \lesssim \frac{1}{2}$. The transport properties have proved to be unexpectedly similar to those of the insulating phase in GaAs/Al_xGa_{1-x}As heterostructures around $\nu=\frac{1}{5}$ (for electron gas) and $\nu=\frac{1}{3}$ (for hole gas) where magnetically induced Wigner solid formation has been reported. Strongly nonlinear current-voltage characteristics display threshold behavior and tend to saturate as current increases. The similarity of transport properties might strongly suggest the formation of a pinned electron solid in Si inversion layers at $\nu \lesssim \frac{1}{2}$. However, in the presence of a long-range potential, at $\nu=\frac{1}{2}$ the percolation metal-insulator transition is expected. Both the magnetically induced electron solid formation and the percolation transition are considered as possible explanations of the observed effects.

I. INTRODUCTION

Investigations of a magnetic-field-induced metal-insulator transition in two-dimensional (2D) electron systems have quite a long history. The transition in extremely high magnetic fields at Landau-level filling factors $\nu<1$ has attracted great interest recently. At sufficiently small ν, the ground state of an ideal 2D electron system is expected to be a Wigner crystal (see, e.g., Refs. 1–5). Another possible ground state in the extreme quantum limit is the electron liquid responsible for the fractional quantum Hall effect (FQHE) at fractional filling factors. The competition between these ground states defines the behavior of the disorderless 2D electron system in high magnetic field.[3–5] Recent theoretical estimates of the critical filling factor ν_c at which the transition from liquid to solid state should occur, give $n_c \approx \frac{1}{6}$,[4] the low disorder at the semiconductor interface leading to higher ν_c as was predicted in Ref. 2. In the case of a strong long-range potential, one can expect magnetic freeze out to occur at ν close to $\frac{1}{2}$.[6]

In the pioneering works[7,8] it has been experimentally shown that in the extreme quantum limit, a magnetic field does promote an insulating phase in silicon metal-oxide-semiconductor field-effect transistors (MOSFET's). Later the peak of experimental activity was transferred to investigations of magnetic-field-induced metal-insulator transition in high-mobility GaAs/Al_xGa_{1-x}As heterostructures at ν about $\frac{1}{5}$.[9–16] This insulating phase was found to be reentrant being interrupted by the FQHE state at $\nu=\frac{1}{5}$. The current-voltage characteristics of the insulating phase were found to be strongly nonlinear.[12,14–16] In the majority of cases, the results have been interpreted as evidence for a pinned electron solid although some doubts in this interpretation were expressed in Ref. 16.

Recently, there has been a revival of interest in the metal-insulator transition in Si MOSFET's.[17–20] Samples with extremely high mobility used in those experiments showed the competition between an insulating phase and the integral quantum Hall effect at $\nu>1$. The transport properties of the solid phase of the 2D electron gas in Si MOSFET's in the low-temperature limit[20] turned out to be very close to those reported for GaAs/Al_xGa_{1-x}As heterostructures around $\nu=\frac{1}{5}$.

At high magnetic fields, the phase boundary between metal and insulator states in the (H,N_s) plane was found to be a straight line with a slope $\partial N_s/\partial H \approx \frac{1}{2}e/hc$.[21] This fact was interpreted as evidence of the percolation character of the metal-insulator transition.

In this paper we report magnetotransport data for the insulating phase in high-quality Si MOSFET's in the extreme quantum limit at $\nu \lesssim \frac{1}{2}$. (We consider a 2D electron system capable of conducting current in a weak electric field at zero temperature to be *metal*. In accordance with this definition the system with zero conductivity σ_{xx} and quantized value of σ_{xy} is a metal. In the insulating phase all the components of a conductivity tensor are equal to zero at $T=0$.)

The results have proved to be unexpectedly similar to those for 2D electron gas at ν around $\frac{1}{5}$ (Refs. 9–16) and hole gas at ν around $\frac{1}{3}$ (Ref. 22) in GaAs heterostructures, as well as for Si MOSFET's in zero and low magnetic field,[18,20] with the exception that the insulating phase was not reentrant below $\nu=\frac{1}{2}$. Strongly nonlinear I-V characteristics with linear $V(I)$ dependence below some threshold voltage V_c and saturation at $V>V_c$ were observed. The similarity of transport properties might

strongly suggest the formation of a pinned electron solid in Si MOSFET's at $\nu \lesssim \nu_c = \frac{1}{2}$. However, this value of ν_c is somewhat surprising since the percolation metal-insulator transition was expected at precisely this filling factor.[6] Both electron solid formation and magnetic freezeout are discussed as possible origins of these effects.

II. EXPERIMENT

Measurements were made on three Si MOSFET's from different wafers. Peak mobilities were $\mu_{\text{peak}} \sim 3 \times 10^4$ cm^2/V s at temperature $T = 1.3$ K. All samples were of the "Hall-bar" geometry (0.25×2.5 and 0.8×5 mm^2) with distances between the nearest potential probes 0.625 and 1.25 mm, respectively. The results obtained for different samples were qualitatively similar.

Magnetotransport measurements were carried out in a dilution refrigerator TLM-400 with a base temperature of ≈ 25 mK. To achieve maximum mobility, the samples were slowly (over 5 h) cooled from room temperature to $T = 1.3$ K with a fixed voltage $V_g = 10$ V between the gate and the 2D layer. This procedure enables us to obtain the most homogeneous distribution of electrons. When measuring the temperature dependences, the temperature at every point was stabilized to make sure that there were no temperature gradients in the mixing chamber. We obtained current-voltage characteristics by measuring the potential difference V between voltage probes when sweeping the source-drain current I_{SD}. At temperatures below 1.3 K and at low electron densities, the contact resistances increased to very high values so that measurements with a standard lock-in technique were no longer possible. All expermental results were obtained by a four-terminal dc technique using two Keithley 614 DVM's as high-input-resistance preamplifiers. Since at low N_s the resistance exceeded 10 GΩ, the source-drain current was set via a resistance of 150 GΩ.

The typical experimental traces are shown in Fig. 1. One can see that at some electron density N_c the nondissipative current through the lower quantum level disappears and the resistivity ρ_{xx} grows abruptly. In high magnetic field the rise of ρ_{xy} starts at lower density than that of ρ_{xx} so that the intersection point of these curves is close to 26 kΩ. The abrupt increase of resistances indicates transition into an insulating phase.

In strong magnetic fields, the metal-insulator phase boundary in (H, N_s) plane has been found to be a straight line with a slope $\partial N_c / \partial H$ close to $\frac{1}{2} e/hc$.[21] The complete phase diagram including low magnetic fields is shown in Fig. 2. The line separating metal and insulator phases is drawn through the points at which the longitudinal resistance per square, R, is equal to $R_c = 100$ kΩ. There are two reasons to consider this value of R_c to be a resistance at which the metal-insulator transition occurs. First, this value is close to the minimum metallic conductivity. Second, the phase boundary determined in this way is nearly independent of temperature. One can see that deviation from the linear dependence begins near the filling factor $\nu = 1$ [the phase boundary at filling factors $\nu > 1$ (see inset in Fig. 2) was investigated in detail in Ref. 17].

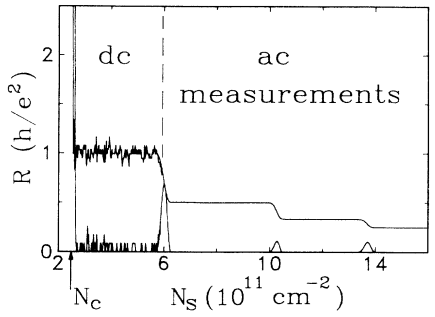

FIG. 1. Experimental dependences of resistivities ρ_{xx}, ρ_{xy} on the electron density. The value of ρ_{xx} is enlarged by a factor of 5. The vertical dashed line separates regions where different experimental techniques were used. $H = 16$ T; $T \approx 100$ mK.

By the triangles in the inset we have shown the experimental points corresponding to $R_c = 500$ kΩ to demonstrate that the overall picture does not depend strongly on the chosen R_c.

Below we show transport data in the high-field, low-ν limit. Typical I-V characteristics normalized per square are shown in Fig. 3 for different H and T. In the vicinity of $I_{SD} = 0$, V is proportional to I_{SD}, while after exceeding some critical value V_c, the voltage remains nearly constant as the current increases further. Both V_c and $\partial V / \partial I$ in the linear part are functions *only* of a point's location in the (H, N_s) plane and are independent of the path taken to this point. The threshold voltages are different for positive and negative I_{SD}: this asymmetry has been discussed in Ref. 18. The threshold voltage can be determined with some accuracy only for temperatures below 200 mK. As the temperature increases, the curves become smooth, and at the temperature $T \gtrsim 300$ mK it is impossible to distinguish a critical voltage at all.

The resistance R corresponding to the linear part of the I-V characteristics displays an activated temperature

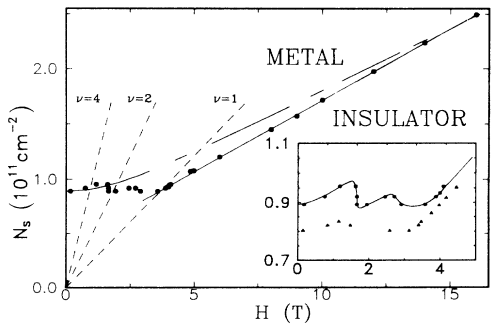

FIG. 2. Phase diagram of metal-insulator transition. Circles are the experimental data taken for $R_c = 100$ kΩ. Dashed lines correspond to filling factors 1, 2, and 4. Dash-dotted line is a fit after Ref. 1. The inset shows, on an expanded scale, the low-field region of the phase diagram. Triangles represent the data determined at $R_c = 500$ kΩ.

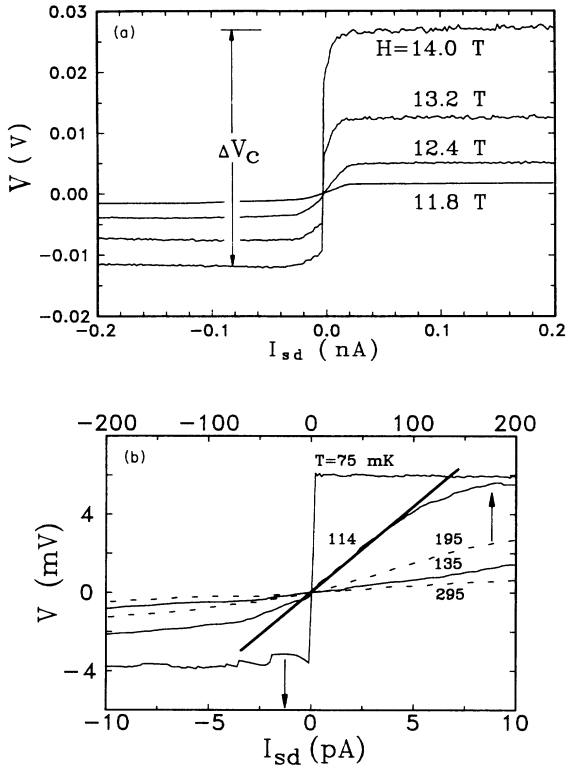

FIG. 3. Typical current-voltage dependences (a) for different magnetic fields at $N_s = 1.86 \times 10^{11}$ cm^{-2} and $T = 70$ mK and (b) for different temperatures at $N_s = 2.1 \times 10^{11}$ cm^{-2} and $H = 14$ T. Dashed lines are referred to upper scale.

dependence (Fig. 4). As long as the resistance is relatively small (less than ~ 10 GΩ), there is no deviation of the experimental points from an Arrhenius law. The last point in Fig. 4 does not fit on the line, probably due to a lack of accuracy in the resistance measurement: The resistance of the sample becomes comparable with the resistance of the dielectric which covers the connecting wires. The preexponential factor is of the order of the minimum metallic conductivity.

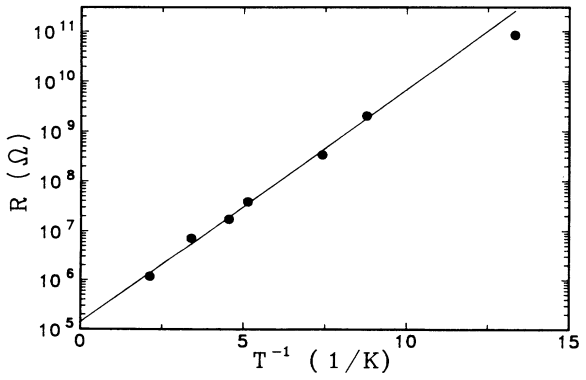

FIG. 4. Arrhenius plot of resistance of the linear part of the I-V curve. $H = 14$ T, $N_s = 2.1 \times 10^{11}$ cm^{-2}.

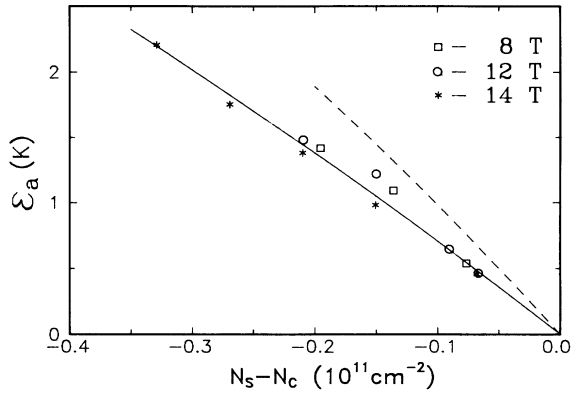

FIG. 5. Activation energy vs electron density for different magnetic fields. Solid and dashed lines are calculated after Ref. 24 for magnetic fields $H = 14$ and 8 T, respectively.

The activation energy increases when moving from phase boundary into the insulating phase, i.e., when increasing the distance between the point and phase boundary in the (H, N_s) plane. An example of this dependence is shown in Fig. 5. The activation energy ε_a is propor-

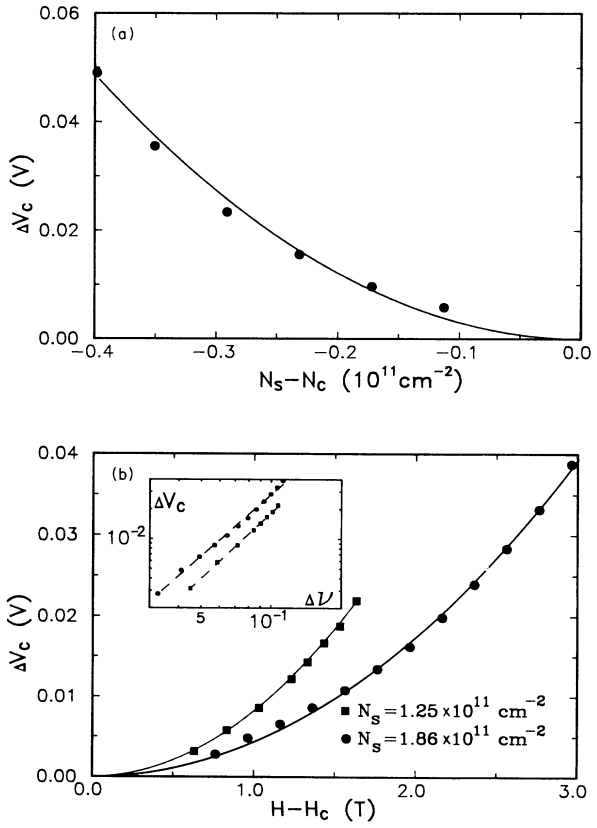

FIG. 6. The dependence of difference between threshold voltages ΔV_c (a) on electron density in fixed magnetic field $H = 14$ T and (b) on magnetic field at fixed $N_s = 1.25$ and 1.86×10^{11} cm^{-2}. Dashed lines in the inset show ΔV_c vs $\Delta\nu = \nu_c - \nu$ with $s = 1.07$ and 1.20 for $N_s = 1.86 \times 10^{11}$ and 1.25×10^{11} cm^{-2}, respectively.

tional to $N_c - N_s$ within the experimental accuracy and tends to zero as the point approaches the phase boundary. The value of the slope of the solid line shown in Fig. 5 is equal to $\partial\varepsilon_a/\partial N_s = 6\times10^{-15}$ cm^2 eV and shows practically no dependence on the magnetic field. For comparison it is interesting to note that the reciprocal of the density of states of a free electron gas in the absence of a magnetic field equals $\partial\varepsilon/\partial N_s = 6.3\times10^{-15}$ cm^2 eV.

The dependences of the difference between the threshold voltages, ΔV_c [see Fig. 3(a)], on the distance from the phase boundary are shown in Fig. 6. Figure 6(a) represents ΔV_c vs $N_c - N_s$ in the magnetic field $H = 14$ T. One can see that this dependence is nonlinear in contrast to linear dependences of the activation energy (Fig. 5). Similar nonlinear behavior is observed when changing the magnetic field at a fixed electron density [Fig 6(b)]. The solid lines in Fig. 6 are a fit to the data using a parabolic law and are guides to the eye only.

In closing this section, we should mention that the FQHE has not been observed at $\nu < 1$ in our samples.

III. DISCUSSION

First of all, we would like to note the astounding similarity of the transport properties of the insulating phase in Si MOSFET's near $\nu = \frac{1}{2}$ and those in GaAs/Al$_x$Ga$_{1-x}$As heterostructures around $\nu = \frac{1}{5}$ (electron gas) and $\frac{1}{3}$ (hole gas). In many papers (see, for example, Refs. 15 and 16) observation of giant nonlinearities has been reported. This phenomenon was related by Jiang *et al.*[16] to the heating of the electron system. In our case, the minimal power at which we have observed voltage saturation ($\lesssim 10^{-13}$ W) seems to be too small for this nonlinearity mechanism to take place; in addition, the power dissipated at the threshold voltage changes strongly for different H or N_s. We shall start by considering the electron solid formation and its depinning in the applied electric field as a possible origin for the observed effects.

A. Electron solid formation

The equations defining the boundary between the electron liquid and the Wigner crystal were found by Lozovik and Yudson.[1] It was shown that in the high-magnetic-field limit this boundary is a straight line in the (H, N_s) plane. Since the transport properties of the insulating phase in the extreme quantum limit are similar to those in the absence of a magnetic field,[18,20] it is reasonable to try to describe the phase boundary by a unified law over the whole range of magnetic fields. Assuming the existence of the electron solid in zero magnetic field,[18,20] we have for the phase boundary[1]

$$l = \gamma r_0 (1 - r_0/r_c)^{-1/4} , \quad (1)$$

where l is the magnetic length, $r_0 = (\pi N_s)^{-1/2}$, r_c is the smallest value of r_0 for which an electron solid still exists in zero field, and γ is a dimensionless parameter (expected $\gamma \sim 0.2$–0.25).[1] The result of calculations of the phase boundary using r_c and γ as fitting parameters is shown in Fig. 2 by the dash-dotted line. The best fit is obtained when $r_c = 1.93\times10^{-6}$ cm and $\gamma = 0.45$. Both values seem to be unrealistic.

In the limit of high magnetic fields, one can expect[1] the phase boundary to correspond to $\nu_c \approx \frac{1}{10}$, contrary to our experimental results. On the other hand, more recent theory yields $\nu_c \approx \frac{1}{6}$.[4] It has been argued in Ref. 2 that low disorder can increase ν_c further, e.g., to $\approx \frac{1}{2}$ for an impurity potential $\sigma = 3\times10^{-4} e^2/\epsilon l^3$ (here ϵ is the dielectric constant). Recently, critical filling factors slightly higher than $\frac{1}{3}$ have been experimentally observed.[22] Narrowing and shift of the cyclotron resonance peak in low density Si inversion layers[23] were interpreted as evidence for the formation of Wigner solid at $\nu \lesssim \frac{1}{2}$.

Assuming that the insulating phase is a pinned electron crystal, the activated temperature dependence of the resistance is a consequence of the gap between the ground and excited states. The value of this gap, $\varepsilon_a \sim 1$ K, is in agreement with that obtained for the insulating phase in GaAs/Al$_x$Ga$_{1-x}$As heterostructures (see e.g., Refs. 9 and 13) and in Si MOSFET's in low magnetic field.[20] The vanishing activation energy near the phase boundary is an indication of the absence of a first-order transition on the boundary line. Chui and Esfarjani[24] have calculated the current transferred by a bound dislocation pair created at finite temperature. In agreement with Ref. 24, the activation energy approaches zero as $\varepsilon_a \propto \nu_c - \nu$. The comparison of experimental results with Ref. 24 is shown in Fig. 5. It should be emphasized that reasonable agreement with experiment can be reached without fitting parameters.

The existence of a threshold voltage in the electron solid phase has been discussed in previous papers (e.g., Refs. 14–16, 18, and 20). The low-electric-field threshold conduction has been considered to be a result of electron solid depinning. As the threshold voltage in our case is of the order of that found in Ref. 20, all the arguments used in that paper are equally valid for the present work and suggest many-particle origin of the threshold conduction. It is interesting that the dependence of ΔV_c on the distance from the phase boundary is close to a parabolic law (solid lines in Fig. 6); overlinear dependence $\Delta V_c(N_s)$ was also observed in Ref. 20.

From the above considerations our results cannot *unambiguously* identify the insulating phase to be a magnetically induced Wigner solid. Furthermore, it is difficult to account for the critical filling factor $\nu_c = \frac{1}{2}$ at $H \to \infty$ since just at this ν the percolation transition is expected in the presence of long-range potential.[6] So, it is necessary to discuss another possibility for explanation of experimental results.

B. Electrons in long-range chaotic potential

In the case of long-range potential fluctuations, the transition curve should be a straight line of slope $\partial N_c/\partial H = \frac{1}{2} e/hc$.[6] This dependence has been found to be valid for all our samples (Fig. 2, see also Ref. 21). The straight line intersects the ordinate axis at the electron density which one can interpret as the number of elec-

trons strongly coupled with positive ions at the interface Si-SiO_2. The density of these ions determined in this way agrees with the results of independent experiments on similar samples.[25]

The activation energy in this model is equal to the energy gap between the percolation threshold and the Fermi level of the electrons localized in potential minima. Hence, in accordance with the experiment, the activation energy should vanish on the phase boundary. In an applied electric field the tilting of the potential relief leads to a shift in the occupied electron states towards the saddle points of the chaotic potential, and at the critical field the area occupied by the electrons is expanded up to saddle points. If we assume the characteristic scale of a cluster to be L then this critical value of the electric field may be estimated as $E_c=\varepsilon_a/eL$. The measured $E_c\sim 10^2$ mV/cm and $\varepsilon_a\sim 1$ K correspond to $L\sim 1$ μm. Near the phase boundary, the cluster dimension diverges as $L\propto(\nu_c-\nu)^{-s}$, where s is a critical index [for 2D system, $s=1.34$ (Ref. 26)]. Taking into account the experimental relation $\varepsilon_a\propto(N_c-N_s)$ (see Fig. 5), one should expect the threshold voltage ΔV_c to be proportional to $(N_c-N_s)^{s+1}$. As can be seen from Fig. 6(a), experimental dependences are close to $\Delta V_c\propto(N_c-N_s)^2$.

A more detailed comparison can be performed using the data shown in Fig. 6(b). The dependence of the threshold voltage ΔV_c on magnetic field at fixed electron density is given by

$$\Delta V_c=\text{const}\times H(\nu_c-\nu)^{s+1} \tag{2}$$

(we have obtained this expression assuming that the number of electrons strongly coupled with positive ions[21] can be neglected and that $\varepsilon_a\propto H-H_c$). The inset in Fig. 6(b) shows the fit to the experimental data using Eq. (2). Two close values of critical index $s=1.07$ and 1.20 are obtained for electron densities 1.86×10^{11} and 1.25×10^{11} cm^{-2}, respectively. The ratio of ΔV_c for these N_s (≈ 1.8) is found to be very close to the ratio of the critical magnetic fields at two electron densities ($=1.73$) in accordance with Eq. (2).

The model of a long-range potential qualitatively explains the experimental results. However, the nature of long-range potential fluctuations in our samples is unclear. It is also hard to explain the sharp threshold on I-V characteristics within this model.

In summary, we have presented a study of electronic transport in a high-mobility two-dimensional system of Si MOSFET's in the extreme quantum limit. In a strong magnetic field, the phase boundary in the (H,N_s) plane has been found to be a straight line with the slope $\partial N_s/\partial H\approx\frac{1}{2}e/hc$ corresponding to $\nu_c=\frac{1}{2}$ at $H\to\infty$. At finite temperature, the transport in the insulating phase is thermally activated. Its activation energy tends to zero at the phase boundary and increases as the electron density decreases.

Current-voltage characteristics reveal several additional features. In the low-temperature limit, we have observed giant nonlinearities in which the voltage saturates as current increases. The threshold voltage was found to be approximately proportional to $(H-H_c)^2$ or $(N_c-N_s)^2$ at constant N_s or H, respectively.

Two possible mechanisms leading to metal-insulator transition have been discussed: the electron solid formation and the percolation transition in a long-range chaotic potential. Each of them can qualitatively explain part of the experimental results; however, it remains to be seen which mechanism really takes place in our samples. The similarity of transport properties of Si MOSFET's at $\nu\lesssim\frac{1}{2}$ and $GaAs/Al_xGa_{1-x}As$ heterostructures around $\nu=\frac{1}{5}$ (electron gas) and $\frac{1}{3}$ (hole gas) strongly suggests the same physical nature of the insulating phases in these systems.

ACKNOWLEDGMENTS

We would like to thank Dr. C. J. Mellor for useful discussions.

[1]Y. E. Lozovik and V. I. Yudson, Pis'ma Zh. Eksp. Teor. Fiz. **22**, 26 (1975) [JETP Lett. **22**, 11 (1975)].
[2]M. Tsukada, J Phys. Soc. Jpn. **42**, 391 (1977).
[3]K. Maki and X. Zotos, Phys. Rev. B **28**, 4349 (1983).
[4]P. K. Lan and S. M. Girvin, Phys. Rev. B **30**, 473 (1984).
[5]D. Levesque, J. J. Weiss, and A. M. MacDonald, Phys. Rev. B **30**, 1056 (1984).
[6]A. L. Efros, in *Proceedings of the 20th International Conference on the Physics of Semiconductors,* edited by E. M. Anastassakis and J. D. Joannopoulos (World Scientific, Singapore, 1990).
[7]S. Kawaji and J. Wakabayashi, Solid State Commun. **22**, 87 (1977).
[8]M. Pepper, Philos. Mag. **37**, 83 (1978).
[9]R. L. Willet, H. L. Stormer, D. C. Tsui, L. N. Pfeiffer, K. W. West, and K. W. Baldwing, Phys. Rev. B **38**, 7881 (1988).
[10]V. J. Goldman, M. Shayegan, and D. C. Tsui, Phys. Rev. Lett. **61**, 881 (1988).
[11]E. Y. Andrei, G. Deville, D. C. Glattli, F. I. B. Williams, E. Paris, and E. Etienne, Phys. Rev. Lett. **60**, 2765 (1988).
[12]R. L. Willet, H. L. Stormer, D. C. Tsui, L. N. Pfeiffer, K. W. West, M. Shayegan, M. Santos, and T. Sajoto, Phys. Rev. B **40**, 6432 (1989).
[13]H. W. Jiang, R. L. Willet, H. L. Stormer, D. C. Tsui, L. N. Pfeiffer, and K. W. West, Phys. Rev. Lett. **65**, 633 (1990).
[14]V. J. Goldman, M. Santos, M. Shayegan, and J. E. Gunnningham, Phys. Rev. Lett. **65**, 2189 (1990).
[15]F. I. B. Williams, P. A. Wright, R. G. Clark, E. A. Andrei, G. Deville, D. C. Glattli, O. Probst, B. Etienne, C. Dorin, C. T. Foxon, and J. J. Harris, Phys. Rev. Lett. **66**, 3285 (1991).
[16]H. W. Jian, H. L. Stormer, D. C. Tsui, L. N. Pfeiffer, and K. W. West, Phys. Rev. B **44**, 8107 (1991).
[17]M. D'Iorio, V. M. Pudalov, and S. G. Semenchinsky, Phys. Lett. A **150**, 422 (1990).
[18]S. V. Kravchenko, V. M. Pudalov, J. Campbell, and M. D'Iorio, Pis'ma Zh. Eksp. Teor. Fiz. **54**, 528 (1991) [JETP

Lett. **54**, 532 (1991)].
[19]S. V. Kravchenko, J. A. A. J. Perenboom, and V. M. Pudalov, Phys. Rev. B **44**, 13 513 (1991); Surf. Sci. **263**, 55 (1992).
[20]M. D'Iorio, V. M. Pudalov, and S. G. Semenchinsky, Surf. Sci. **263**, 49 (1992); S. V. Kravchenko, Jos A. A. J. Perenboom, and V. M. Pudalov, Phys. Rev. B **44**, 13 513 (1991).
[21]V. T. Dolgopolov, G. V. Kravchenko, and A. A. Shashkin, Pis'ma Zh. Eksp. Teor. Fiz. **55**, 146 (1992) [JETP Lett. **55**, 140 (1992)].
[22]M. B. Santos, Y. W. Suen, M. Shayegan, Y. P. Li, L. W. Engel, and D. C. Tsui, Phys. Rev. Lett. **68**, 1188 (1992).
[23]B. A. Wilson, S. J. Allen, Jr., and D. C. Tsui, Phys. Rev. B **24**, 5887 (1981).
[24]S. T. Chui and K. Esfarjani, Phys. Rev. Lett. **66**, 652 (1991).
[25]E. A. Vyrodov, V. T. Dolgopolov, S. I. Dorozhkin, and N. B. Zhitenev, Zh. Eksp. Teor. Fiz. **94**, 234 (1988) [Sov. Phys. JETP **67**, 998 (1998)].
[26]B. I. Shklovskii and A. L. Efros, *Electronic Properties of Doped Semiconductors* (Springer, New York, 1984).